A Fast Single-Pixel Laser Imager for VR/AR Headset Tracking

Veljko Milanović*, Abhishek Kasturi, James Yang, Frank Hu

Mirrorcle Technologies, Inc., Richmond, CA

ABSTRACT

In this work we demonstrate a highly flexible laser imaging system for 3D sensing applications such as in tracking of VR/AR headsets, hands and gestures. The system uses a MEMS mirror scan module to transmit low power laser pulses over programmable areas within a field of view and uses a single photodiode to measure the reflected light. User can arbitrarily select the number of pixels to scan over an area and can thus obtain images of target objects at arbitrarily fast rates. The work builds on the previously presented "MEMSEye" laser tracking technology which uses a fast steering MEMS scan module with a modulated laser, and a tuned photosensor to acquire and track a retroreflector-marked object. To track VR/AR headsets, hands and similar objects with multiple markers or no markers at all, a single-point tracking methodology is not sufficient. Cameras could be more appropriate in such multi-point imaging cases but suffer from low frame rates, dependence on ambient lighting, and relatively low resolution when without zooming and panning capability. A hybrid method can address the problem by providing a system with its own light source (laser beam), and with full programmability of the pixel locations and scans such that frame rates of >100 Hz are possible over specific areas of interest. With a modest 1 Mpixel rate of measurement, scanning a sub-region of the field of view with 64 x 64 pixels results in ~200Hz update. Multiple such modules can be used to scan and image or track objects with multiple markers and fully obtain their position and attitude in a room with sub-5ms updates. Furthermore the room itself could be imaged and measured with wall markers or in conjunction with a camera for a total 3D scanning solution. Proof of concept demonstrator is presented here with pixel rates of only 30k-50k per second due to limitations of the present prototype electronics, resulting in refresh rates that are significantly lower than possible with the MEMS mirror scan modules.

Keywords: single-pixel camera, laser imaging, MEMS Mirror, beam-steering, 3D tracking, 3D imaging, real-time tracking, retro reflector, VR (Virtual Reality), AR (Augmented Reality).

1. INTRODUCTION

Obtaining real-time 3D coordinates of a moving object has many applications such as gaming [1] including VR, robotics and human-computer interaction [2]-[4], industrial applications and others. Various technologies have been investigated for and used in these applications, including sensing via wire-interfaces, ultrasound, cameras and other optical measurements. A simple and low-cost solution that can provide enough precision and flexibility and high update rates is not yet available as each solution comes with associated trade-offs. In 2011 we presented the MEMSEye utilizing scanning MEMS mirrors as technology platform to build a high resolution and high speed 3D position measurement system [5]. The concept involved two MEMS-based laser trackers that were used to track and triangulate the position of an object with a high-contrast retro-reflective marker. This technology was used e.g. to build a wind turbine blade tracking system where a retro-reflective marker could be tracked with high speed and accuracy at >50m distance, continuously reporting blade deformation.

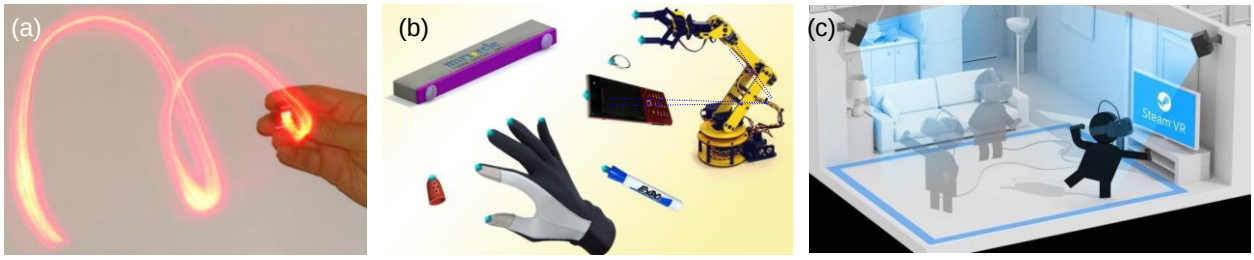

Figure 1. Optical tracking of objects in robotics, gaming, and other applications: (a) MEMSEye laser tracker [5] points the tracking laser beam at the corner-cube held by hand in this example and follows the corner-cube at very fast rates of movement. (b) We depict various possible system uses based on where we attach the small tracking targets. For example, robot's end effector position is monitored. (c) Steam VR concept for VR environments where multiple optical sensors are tracking multiple user's VR headsets and controllers. Obtained by permission from [18]

Positional trackers are key factors to the VR/AR experience. In order to accurately detect the position and orientation of a head-mounted display (HMD) or handheld devices for VR/AR applications, modern position trackers implement a variety of sensors that report the measured position and orientation and accordingly update the virtual environment. This is depicted in the Steam VR concept shown in Figure 1c. These sensors use different methods of receiving position and orientation information. Common sensor types include acoustic, inertial, magnetic, mechanical and optical. Each one of these comes with advantages and disadvantages. Metrics such as accuracy, resolution, refresh rate, latency and operating environment can be used to compare the effectiveness of a sensor. A good position tracker should have high accuracy, fine resolution and high update rate. Its latency should be low and its working volume should be large. Ideally, it should not need any specialized environment for operation. In addition, the parts of the tracker that need to be worn should be small and light in weight, to ensure user comfort. Within the past few years, virtual reality (VR) and augmented reality (AR) systems have become smaller, lightweight, and more affordable for mainstream consumers [1].

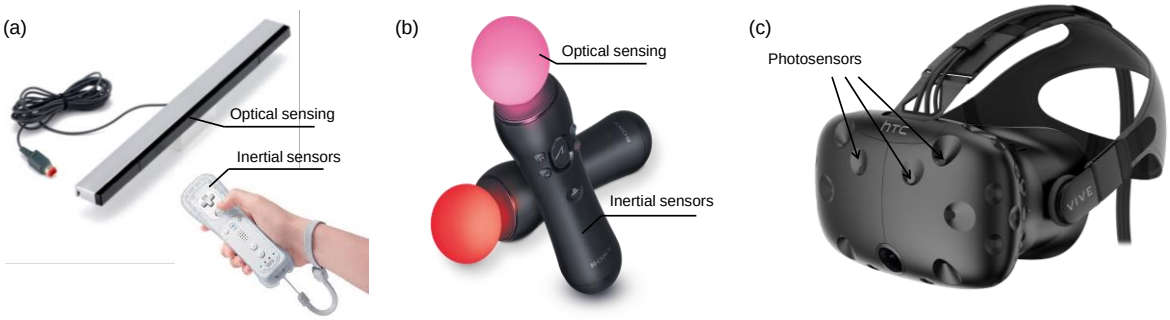

Figure 2. 3D Sensing in gaming and other AR/VR applications: (a)Wii remote and sensor bar to optically track the controller with an inertial sensor, (b) Handheld controllers with built-in inertial and optical sensors (c) VR headsets with photodiodes or retro-reflective markers for position and orientation tracking.

One of the first influential consumer products interfacing and representing real 3D environments was the Nintendo Wii, which used inertial sensors and infrared LEDs to roughly track the position and orientation of handheld controller devices. The Wii gaming system is widely considered a breakthrough in the game controller design, as it not only allows free movement for the user, but also makes use of that movement for user to interact with the virtual world. The controller (Figure 2a) tracking system utilizes a single camera-based IR position sensing system and three-axis accelerometers. An IR emitter bar is placed in front of the user, emitting from two IR sources a known distance apart. The handheld sensor images the sources onto a camera at standard camera rates (tens of milliseconds for update). Following the Wii, Microsoft released the Kinect which used cameras and depth sensing to capture 3D motion and convert it to actions in games. Despite the success of both these products, their positional tracking lack requirements to fully immerse the user within a virtual or augmented reality.

Similarly, compact and lightweight acoustic trackers such as the Ultrahaptics sensor uses time of flight or phase coherence to determine 3D position, but disadvantages include low update rates as well as being error-prone from noise and reflections [6].

Inertial sensors are popular due their small size and low price. They are mostly used in hybrid with other sensors in many current VR/AR systems. These sensors are quite accurate and have high update rates and low latency but are known to have drift error. A common setup includes pairing inertial sensors with optical trackers such as those in HTC's Lighthouse (Figure 2c). Namely an optical tracker would be necessary to provide absolute position data to correct or supplement the integrated position data from inertial sensors which would otherwise drift beyond usability.

Therefore a solution based on the MEMSEye work is proposed to track objects marked with retro-reflective markers. The MEMS mirror technology utilized in MEMSEye has been used in other established applications such as 3D scanning, LiDAR [16], etc. Within the field of AR/VR, MEMS mirrors are not just limited to headset / user tracking. MEMS mirrors can be used for eye tracking, and projecting content directly to the eye using pico-projection technology [17].

2. SINGLE-PIXEL LASER IMAGER

Laser beam-steering based imaging is widely used in biomedical applications. Due to many desirable properties like high brightness, stability, longevity and narrow spectral bandwidth, lasers are increasingly replacing conventional, broadband light sources in e.g. fluorescence imaging applications. Lasers allow for higher-sensitivity visualization and enhanced throughput in many imaging applications. Some key properties of lasers include narrow beam divergence, a high degree

of spatial and temporal coherence and well-defined polarization properties enabled new fluorescence imaging techniques. At the same time, the use of lasers as fluorescence light sources imposes new constraints on imaging systems and their components. For example, optical filters used in laser-based imaging systems such as confocal and Total Internal Reflection Fluorescence (TIRF) microscopes [7] have unique requirements compared to filters used in broadband light source-based instruments.

In the optical coherence tomography (OCT) 3D imaging methodology [8]-[10], the laser beam-steering system performs the so-called "B" and "C" scans which determine which portion of the sample is depth-imaged. In many of the methodologies of laser based imaging there is an image reconstruction with a number of rows and pixels per row although there is no array of pixels utilized. Instead, a single photosensor such as a simple silicon photodiode is obtaining optical measurements at each target location that the beam points to in a time-sequence.

This simple principle of imaging has some obvious advantages and drawbacks when compared to camera based imaging. One of the major advantages is naturally that it inherently provides illumination for the target object, and more specifically for the local region of the target pixel. Therefore it is insensitive to ambient lighting conditions. Furthermore the illumination is very strong and fully localized to the target location which means that a high sensitivity is possible with low power consumption. Another advantage is that the actual array of reconstructed pixels in the image can be flexibly arranged based on the scan and sampling algorithm. For example an image of 1000x500 pixels may be obtained by scanning 500 lines over a target area or an image of 300x100 pixels by scanning 100 lines, etc.

Disadvantage comes from the fact that the data is obtained sequentially, point by point, at different relative times instead of simultaneously. For images that require a very large number of lines as possible, cameras with the time to acquire complete images could easily exceed the time used by cameras for integration. Therefore there is a direct trade-off between the number of lines versus the refresh-rate of the system.

The imaging system is arranged in such a way that a photosensor is placed in close proximity to the scanned laser source, with both facing toward the target area. In this case the signal that is detected by the photosensor at each target location pointed by the laser beam is the retro-reflected light from the target. If the target is highly dispersive the laser beam is nearly equally reflected in all directions and only low reflection would be detectable through the photosensor's receiving aperture. Thus received laser power drops quadratically with distance. On the other hand, if the target is highly retro-reflective, for example if it includes highly efficient retro-reflective markers or corner-cubes, then a very high percentage of the transmitted laser beam can be received at the receiver and a much lower distance dependence is found. In such cases distances of tens of meters are possible with a simple eye-safe system.

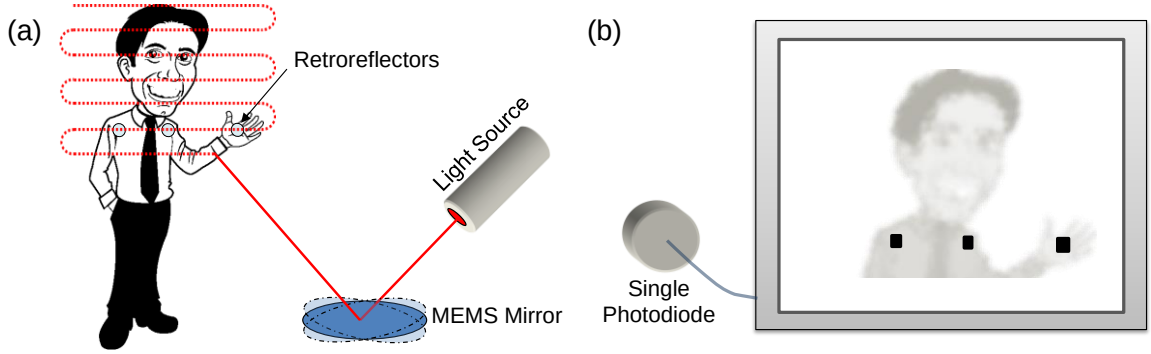

Figure 3. Testing setup for position tracking: (a) A MEMS mirror steers a light source in a raster pattern across the field of regard, (b) A single photodiode measured the returned light at each point and displays the reflected intensity on a screen.

3. ZOOM, OFFSET, TRACKING

As mentioned in the previous section, having a laser beam-steering system and a single photosensor allows for very flexible imaging. The number of lines, pixels along a line and the scan area can arbitrarily be controlled provided the beam-steering system allows for such programmability. In our case we utilize two-axis quasistatic MEMS mirrors to have this arbitrary pattern flexibility. The ultimate limit is based on the optical resolution considerations of the transmitted beam, i.e. considering how small of an area in a target field of view the beam can address. For the highest "zoom-in" capability it would be ideal to have this area as small as possible, i.e. a laser beam of small diameter and smallest possible divergence. However there are cases where the opposite would be useful as well, e.g. to obtain quick

preview scans of a wide field of view with few lines and pixels – here a large beam divergence would work best to fully cover the region with less lines, however it would trade off power density. For this option it would be ideal to have a programmable beam divergence by the use of a controllable lens in the optical cell.

With a line time of e.g. 0.0005s, scanning 20 lines results in 100Hz refresh rate while scanning of 200 lines results in 10 Hz. Although quasistatic-capable mirrors have relatively lower resonant frequencies, there are still many designs with >5kline/s rates. In this case with 0.0002s per line, measuring 25 lines is possible at 200Hz. In the examples shown in Figure 5, the MEMS mirror scans a 12° x 12° field of regard with 48 lines, and a refresh rate of 52Hz. The same number of lines and refresh rate is then offset and scanned over a smaller area of approximately 9° x 9°, increasing the density of the points sampled in the given area. Figure 5c demonstrates the ability of the MEMS mirror to offset and rotate the raster scan angle, and still be able to perform the same measurements.

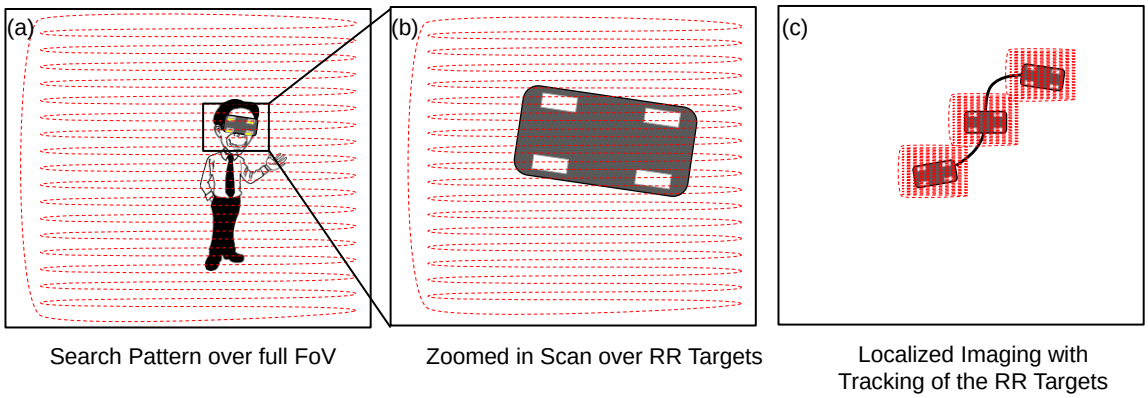

Figure 4. (a) A scan of the full Field of View (FoV) to image and detect any retro-reflective (RR) targets, (b) the same resolution and refresh rate is used to zoom in to the area around the headset with the RR targets, (c) While maintaining the zoomed in scan, the VR headset is tracked by offsetting the position of the scan after each frame – updating the position of the scan at the refresh rate.

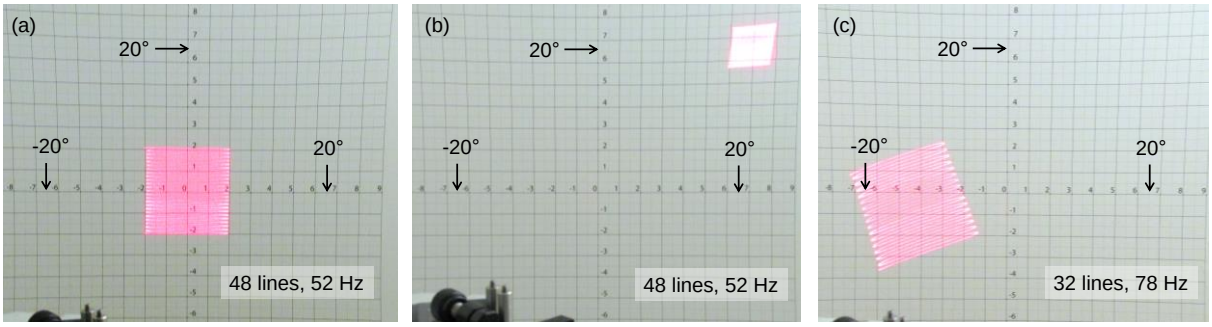

Figure 5. The reference graph shown behind the scan has each unit increment representing 3° optical degrees. (a) Example of a raster scan with 48 lines, scanning at 52 Hz, over a 12° x 12° area, (b) The same resolution of the scan, with 48 lines updating at 52 Hz refresh rate is offset to +20° on X-axis and +20° on Y-axis, and scanning a FoV of +/-6°, (c) An example of a raster scan that is rotated at 20° and offset to -12° on X-axis, and -2° on Y-axis, scanning 32 lines at 78 Hz.

The MEMS mirror can address the entire field of regard, or any sub-region within the field of regard, with an arbitrary number of lines, offset and orientation of the line scan. This quasi-static mode of driving of the MEMS mirror can be combined with the single-pixel camera sensor to image the field of regard (Figure 4a), zoom in to any areas with retro-reflective markers (Figure 4b), and track the markers by adjusting the offset of the raster scan at each pass (Figure 4c). The scanner can continue tracking the target as it moves anywhere within the overall field of regard of the single-pixel camera.

4. MEMS BASED LASER IMAGING MODULE

4.1 MEMS MIRROR

To achieve a laser-scanning module with a lot of flexibility, we targeted a device design with point-to-point or quasi-static two-axis beam steering capability with significant tip/tilt angle and with a high frequency response bandwidth. We utilized gimbal-less two-axis MEMS beam-steering mirrors based on monolithic, vertical combdrive actuators [11]-[14]. The gimbal-less design results in fastest two-axis beam steering with large optical deflections of >20° over the entire device bandwidth, from DC to several kHz for the chosen 1.2mm diameter mirror size. The capability for equally fast beam steering in both axes is a great match for use in laser tracking, laser marking, 3D printing applications, as well as present work displaying vector graphics. We had previously demonstrated a highly adaptive MEMS-based display [15] and its application for windshield HUDs using a similar integrated MEMS mirror with 0.8mm diameter mirror.

The MEMS mirror device (Figure 6a) is made entirely of monolithic single-crystal silicon, resulting in excellent repeatability and reliability. Flat, smooth mirror surfaces are coated with a thin film of aluminum with high broadband reflectance in the visible red wavelengths. Flatness of the final, metalized and packaged mirrors is tested on a WYKO NT3300 interferometer. Most mirrors measure between 7m to 10m radius of curvature. With such high flatness and surface roughness below 5nm, the mirrors are highly suitable for any laser beam steering application. Another important benefit of electrostatic driving and pure single-crystal silicon construction is an exceptionally wide range of operation temperature. We have demonstrated normal operation at up to 200°C [14].

As mentioned above, the design is focused on wide bandwidth to allow the laser beam scan to directly follow arbitrary voltage commands on a point-to-point basis. A fast sequence of actuation voltages results in a fast sequence of angles for point-to-point scanning. There is a one-to-one correspondence of actuation voltages and resulting angles: it is highly repeatable with no detectable degradation over time. For devices with mechanical tilt range of -5° to +5° on each axis, tilt resolution (repeatability of steering to a specific angle over an extended period of time) is within 0.6 milli-degrees or within 10 micro-radians. The desired trajectories must be pre-conditioned in order to limit bandwidth of the waveform reaching the device and to prevent oscillations [13]. This is done firstly by time-domain input shaping of the vector content acceleration/constant velocity/deceleration control during interpolation. Then it is also done in frequency domain by filtering out the content that would excite the high quality factor resonant response seen in Figure 6c. As described in [12], we utilized a digital IIR inverse filter, and increased the bandwidth of the MEMS device from ~4 kHz to ~8 kHz.

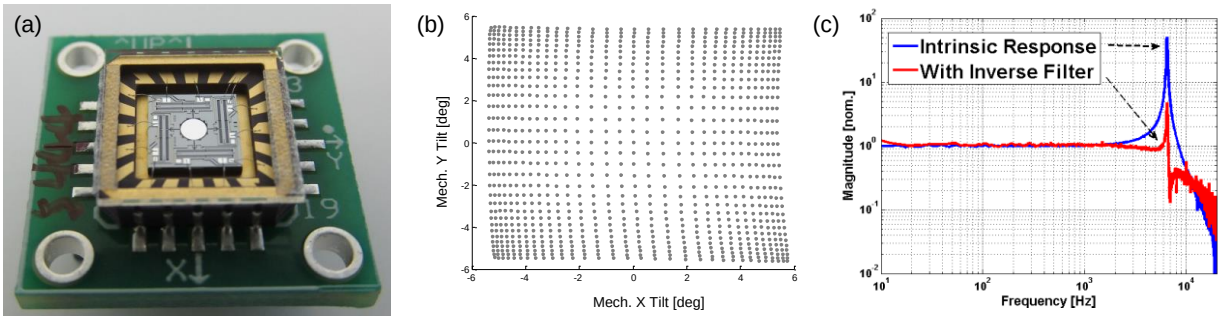

Figure 6. MEMS Mirror Device used in this work: (a) Photograph of the A3I12.2 MEMS device packaged in a 9mm wide ceramic carrier, (b) 2D look-up table (LUT) of the X and Y mechanical tilt recorded on a PSD. The optical distortions seen on the LUT are due to 22.5° angle of incidence of the scanning laser on the MEMS device. (c) Intrinsic frequency response of a device with a 6200Hz resonance and frequency response of the device with inverse filtering applied.

To actuate the rotating bi-directional electrostatic combdrives, we utilize a "push-pull" method of driving with a Bias-Differential Quad-channel (BDQ) scheme [13]. This scheme linearizes actuators' voltage-angle relationship and improves smooth transitions from one quadrant to another, i.e. from one actuator to another within the device. In this mode both the positive rotation portion and the negative rotation portion of each rotator are always differentially engaged. Specifically, we bias all of the moving sections of the combdrives with 80V with respect to stators. Then, in response to user commands for mirror tilt, one section is given additional voltage and the opposite-acting section reduced voltage. Driving the MEMS mirror to full tip/tilt angles on both axes (4-quadrants) therefore utilizes four high voltage channels with 0 to ~160V output range.

4.2 MEMS SCAN MODULE

The MEMS mirror is the main component of the laser scanning system, but in addition to the MEMS, a light source, beam shaping optics, and scanning optics are put together in an opto-mechanical assembly. The opto-mechanical assembly began with off-the-shelf lenses and optical breadboard components, and eventually reduced in size to a 3D printed optical cell (Figure 9b). The cell consisted of a red laser (635nm) with a collimation lens and a positive lens to

reduce the laser beam size to fit onto the MEMS device. After the MEMS device, a negative lens is used to re-collimate the beam, as it exits the cell.

Since the optical scanning angle of our MEMS mirror is -10° to +10°, the wide angle (negative) lens also increases the overall field of view to ~40°. As seen in Figure 7, the MEMS mirror is placed in between the positive lens element and the negative lens element which together form the beam-reducer that increases the scan angle by approximately 2X. The complete optical cell can be reduced in size and formed out of simple spherical off-the-shelf lens elements as seen in Figure 9b, and held in place by machined or 3D printed cell housing.

The 40° scanning capability comes with inherent pin-cushion distortion. In addition to that, any misalignment of the optics and the MEMS mirror as well as some F-Theta nonlinearity results in a non-ideal scan field of the light engine. The MEMS device's static response has nonlinearity at larger angles in the device as well adding to the complexity of the final relationship between input commands and output beam location. Here we find another major advantage of vector graphics methodology, namely that it allows us to practically eliminate all of these distortions by allowing the user to fully control the beam position and velocity and therefore to correct any amount of optical field distortion either computationally by model or by actual measurement/calibration [12]. We have successfully demonstrated correction of major non-linearities in the projection lens, MEMS device, as well as correction of perspective angles when projecting content onto non-normal surfaces in the past, and have integrated these correction capabilities into our light engine control software. Ultimately, a complete unit-specific look up table can be created during production/calibration that fully eliminates beam pointing errors.

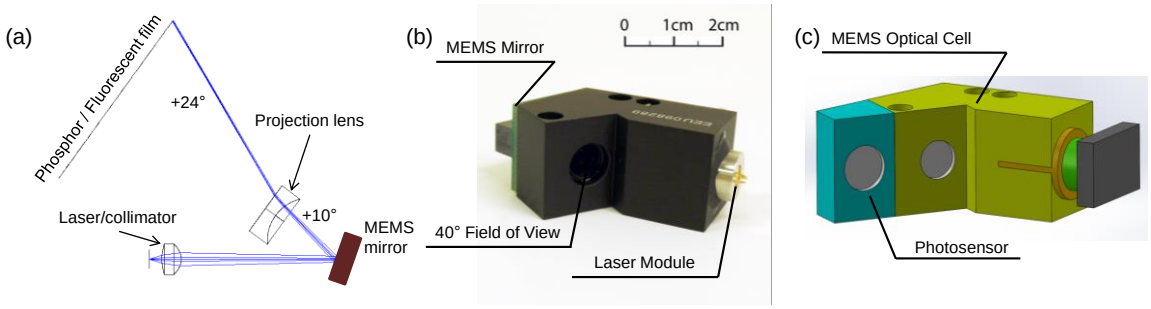

Figure 7. MEMS Scan Module design: (a) Schematic of design for increased field of view scanning. Laser diode is collimated and the beam is then reduced by a convex-concave lens beam reducer. MEMS mirror is placed between the beam reducer lenses, scanning the beam over the concave lens which increases the scanning angle and re-collimates the beam. (b) Current MEMS optical cell in an aluminum body, (c) Prototype MEMS Scan Module with off the shelf optics and two separate apertures for out-going scanning beam, and receiver for any reflected light for the photosensor.

4.3 MEMS DRIVER AND CONTROLLER

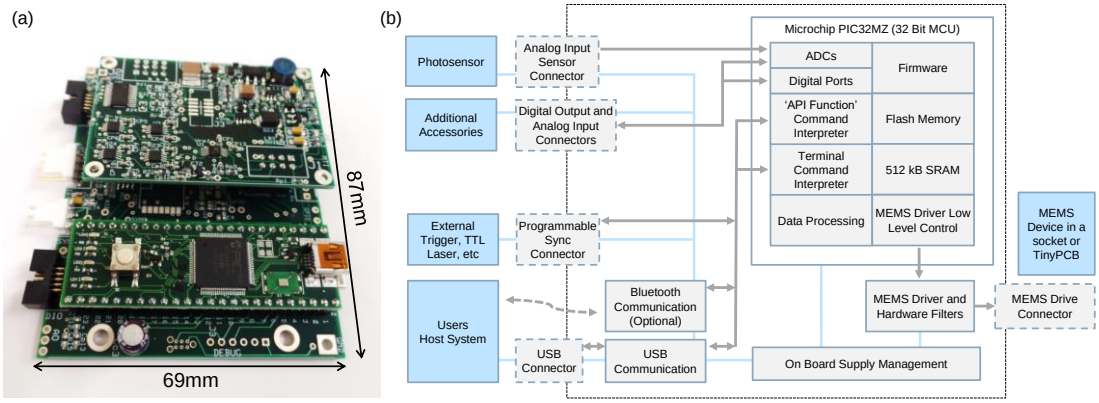

Figure 8. USB-SL MZ MEMS controller: (a) The development kit controller measures 69mm x 87mm, (b) Diagram of controller

The bare minimum of electronics needed in order to drive the MEMS device is a MEMS driver. Simple analog voltages from a function generator, signals generated by DAQ cards, or even digital SPI signals from a microcontroller, FGPA, etc. can provide content to the MEMS driver. For demonstrating the single-pixel camera concept, a "USB-SL MZ MEMS Controller" was used which contains a fast microcontroller, with USB and Bluetooth interface, and an embedded

"PicoAmp" MEMS driver (Figure 8a). The PicoAmp is a quad-channel 16-bit high voltage driver with SPI digital input and programmable hardware filtering. The MEMS driver runs on a +5VDC power supply and ~25mA of current in active state. The USB controller is flashed with a firmware that can interface with a host through a C++ based Windows API (application programming interface), Java based Android API, or by serial terminal commands, either via USB cable or wirelessly via Bluetooth. The MEMS device can be controlled from a host PC, a mobile device, or other development platforms such as Raspberry Pi or Arduino. The USB controller was primarily designed for development purposes, and comes with additional connectors for analog inputs, digital outputs, a port for inputting or outputting trigger signals, and an analog input for a photosensor (Figure 8b).

The MEMS mirror's scanning content is generated on a host using the provided software development kits and API or fully built applications. For example, the MirrorcleDraw software allows the user to draw arbitrary freehand or line sketches and compose various parametric mathematical curves. It is also possible to input text or to load multi-frame animations consisting of lists of keypoints for each frame with MirrorcleDraw. The API allows users to generate any type of content using provided functions or importing scan path data. The raw data is then interpolated to the system's sample rate in a way that maximizes the laser on time, resulting in 80%-85% usage of available laser power. Lastly the software has the option of digital filtering to the sample content to optimize the driving voltages for the device's dynamics.

4.4 PROOF-OF-CONCEPT SYSTEMS

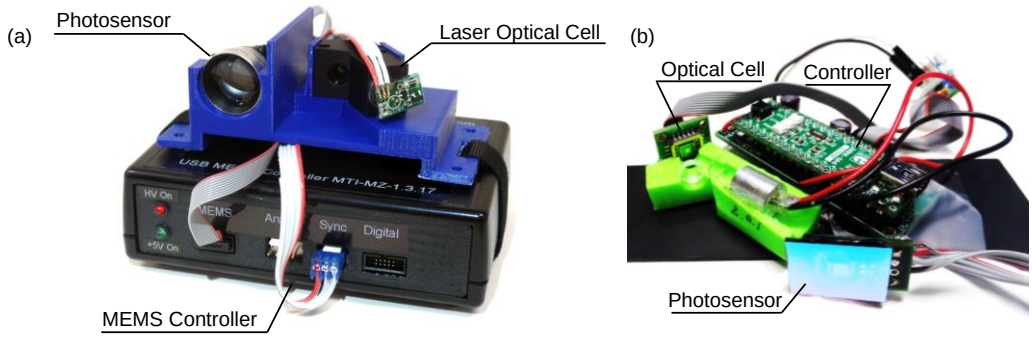

Figure 9. (a) Laser Tracking and MEMS Mirror Demonstrator Kit controller, with the laser optical cell and photosensor, (b) A reduced size, weight, and power consuming version of the MEMS controller with optical cell and photosensor.

To demonstrate the single-pixel camera with the MEMS mirror, we used a USB-SL MEMS controller with a pre-assembled laser scan module. The scan module comprises of a 1.2mm diameter mirror MEMS device and a photosensor. The photosensor is constructed with a silicon photodiode and transimpedance amplifier circuit, and is optically filtered with a red band pass filter. The field of view of the sensor is reduced to 60° by using a cellphone camera telephoto lens (Figure 9a). To make the system compact and portable, the photosensor and MEMS scan module were assembled together on a 3D printed cradle that sits on top of the USB-SL MEMS controller. This system was used to scan and image various objects, and track objects marked with retro-reflective markers. The following Results section presents the achievements of this system.

Since the system is made of three individual components, each of them can be modified to improve in various categories such as size, weight, power consumption, etc. For example, the system shown in Fig 9b was optimized to consume less power and be light enough to fly on a toy drone, and eventually for UAV LiDAR applications [16]. The controller is stripped down to the core components of a processor, driver and Bluetooth transceiver for communication, removing any additional peripherals available in the development kit, and removing the plastic housing. The optical cell is made from light weight 3D printed plastic instead of Aluminum housing. All three of these components added up to only 40g in weight, and are able to run directly from the drone's battery without significantly reducing the drone's battery life (Figure 9b).

5. RESULTS

We have demonstrated a MEMS laser scanner based single-pixel camera which addresses a 40° field of regard with an eye-safe laser beam and can be used to display and annotate, image, and track targets. The scan module with photosensor can be less than 40g in weight, fits in a volume of <70mm x 40mm x 35mm. The MEMS controller and

driving electronics can fit within a 40mm x 60mm PCB. The total laser scanning and imaging system weighs 200g, and consumes less than 1W of power. This single-pixel camera has demonstrated that it can image up to 12 kLines / Second using the A7M8.1 MEMS mirror, 0.8mm diameter integrated Aluminum mirror. The single-pixel camera was successfully used to image and display any object within 1 meter distance. Figure 10 shows examples of hands and face being imaged by the single-pixel camera system. The system was successful in imaging and detecting retro-reflective ping pong balls, VR headsets with retro-reflective markers up to ~12m. Figure 11 shows the laser scanning over the VR headset with retro-reflective markers, and displaying the position of the markers at various distances. The position and orientation of the VR headset can be determined by the position of the constellation of markers on the VR headset. The single-pixel camera was successfully able to image and track retro-reflective marked objects up to ~8m away by zooming into the area around the target as it moved farther away. The camera can scan and image the entire field of regard of 40° or scan selected regions to locally increase resolution. Figure 12 shows the camera detecting a small grouping of pixels 5m away as a retro reflective target, and zooming into to resolve the grouping to a 30 x 30 pixel image of the letter "A" at 30Hz refresh rates.

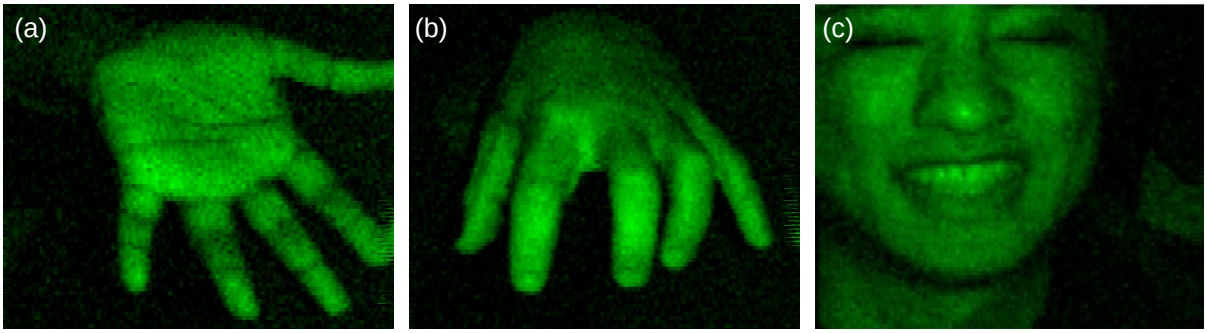

Figure 10. (a) The single-pixel camera imaging a hand ~1m in front, with 60 lines, and 16 Hz refresh rates, (b) Another image of a hand with the same resolution, (c) an image of a face scanned ~1m in front of the imager.

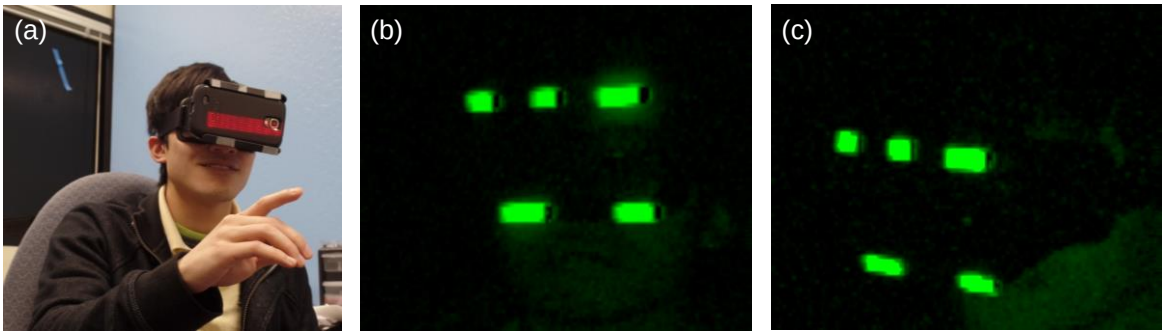

Figure 11. (a) The single-pixel camera raster scanning over the VR headset with retro-reflective markers, (b) a zoomed scan of the 5 RR markers on the VR headset, (c) Another frame of the zoomed scan of the VR Headset with the head tilted and rotated to a different position. The location of the constellation of RR markers can be used to determine 3D orientation and position of the VR Headset.

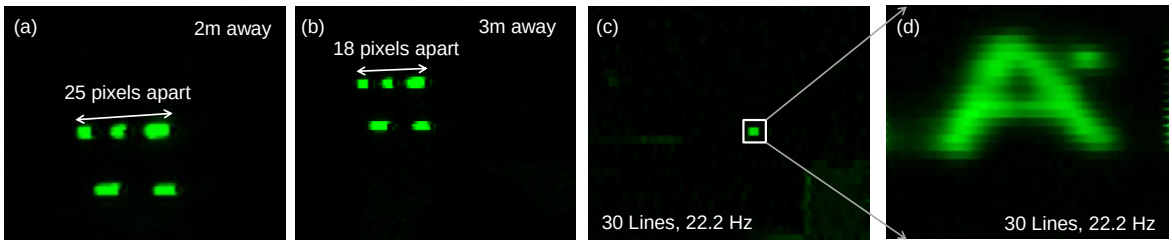

Figure 12. (a) A frame of the zoomed scan of a VR Headset with RR markers approximately 2m away from the imager, (b) A frame of the zoomed scan of a VR headset ~3m away, and the difference in distance between the markers in Fig12a compared to Fig12b can be used to determine depth information. (c) A scan of the 5° x 5° FoV, with 30 lines at 22.2 Hz, in front of the imager, where a few pixels identify a RR target, (d) A ~0.1° x 0.1° zoomed in scan of the RR target identified in c, with the same resolution.

6. ACKNOWLEDGEMENT

The authors thank John Haroian and Donald Humbert of Microchip Technology, Inc. for the development and integration of the PIC32MZ processor into the new USB-SL MEMS Controller.

7. REFERENCES

[1] Axworthy, J., "The origins of virtual reality", http://www.wareable.com/wearable-tech/origins-of-virtual-reality-2535.
[2] Brophy-Warren, J., "Magic Wand: How Hackers Make Use Of Their Wii-motes," The Wall Street Journal, Apr. 28th, 2007.
[3] Arcara, P., et al, "Perception of Depth Information by Means of a Wire-Actuated Haptic Interface," Proc. of 2000 IEEE Int. Conf. on Robotics and Automation, Apr. 2000.
[4] Aoyagi, S., et al. "Measurement of 3-D Position and Orientation of a ROBT using Ultrasonic waves", CH2976-9/91/0000-2466, IEEE 1991.
[5] Milanović, V., Siu, N., Kasturi, A., Radojičić, M., Su, Y., ""MEMSEye" for Optical 3D Position and Orientation Measurement," Proc. SPIE 7930, MOEMS and Miniaturized Systems X, 7930-27, March, 2011.
[6] Bhatnagar, D. K., "Position trackers for Head Mounted Display systems: A survey." http://www.cs.unc.edu/techreports/93-010/93-010.pdf, Mar. 1993.
[7] Huang, X., "MEMS-Based Shadowless-illuminated variable-angle TIRF (SIVA-TIRF)," in CLEO: 2015, OSA Technical Digest, paper ATh1J.3, Optical Society of America, 2015.
[8] Nankivil, D., Waterman, D., LaRocca, F., Keller, B., Kuo, A.N., Izatt, J.A., "Handheld, rapidly switchable, anterior/posterior segment swept source optical coherence tomography probe," Biomed. Opt. Express 6, 4516-4528 (2015)
[9] Canavesi C., Cogliati, A., Hayes, A., Santhanam, A.P., Tankam, P., Rolland, J.P., " Gabor-domain optical coherence microscopy with integrated dual-axis MEMS scanner for fast 3D imaging and metrology ", Proc. SPIE 9633, Optifab 2015, 96330O (October 11, 2015)
[10] Lu, D. C., Kraus, M. F., Potsaid, B., Liu, J. J., Choi, W., Jayaraman, V., Cable, A.E., Hornegger, J., Duker, J.S., Fujimoto, J.G., "Handheld ultrahigh speed swept source optical coherence tomography instrument using a MEMS scanning mirror," Biomed. Opt. Express 5, 293-311 (2014)
[11] Milanović, V., Matus, G., McCormick, D.T., "Gimbal-less Monolithic Silicon Actuators For Tip-Tilt-Piston Micromirror Applications," IEEE J. of Select Topics in Quantum Electronics, vol. 10, no. 3, pp. 462-471, Jun. (2004).
[12] Milanović, V., Castelino, K., "Sub-100 µs Settling Time and Low Voltage Operation for Gimbal-less Two-Axis Scanners," IEEE/LEOS Optical MEMS 2004, Takamatsu, Japan, Aug. (2004).
[13] Milanović, V., "Linearized Gimbal-less Two-Axis MEMS Mirrors," 2009 Optical Fiber Communication Conference and Exposition (OFC'09), San Diego, CA, Mar. 25, (2009).
[14] Miner, A., Milanović, V., "High Temperature Operation of Gimbal-less Two-Axis Micromirrors," 2007 IEEE/LEOS Optical MEMS and Their Applications Conf., Hualien, Taiwan, Aug. 12, (2007).
[15] Milanović, V., Kasturi, A., Hachtel, V., "High brightness MEMS mirror based head-up display (HUD) modules with wireless data streaming capability ," SPIE 2015 OPTO Conference, San Francisco, CA, Feb. 2015
[16] Kasturi, A., Milanović, V., Atwood, B.H., Yang, J., " UAV-Borne LiDAR with MEMS Mirror Based Scanning Capability ," SPIE Defense and Commercial Sensing Conference 2016, Baltimore, MD, April 20th, 2016
[17] Lang, B., "Exclusive: Former Oculus VP of Engineering Demonstrates Long Range VR Tracking System." http://www.roadtovr.com/mts-virtual-reality-vr-tracking-system-jack-mccauley-oculus-vp-engineering/
[18] Prasuethsut, L., "HTC Vive Review," https://www.wareable.com/vr/htc-vive-review.